Journal of Engineering Science and Technology
Vol. 18, No. 1 (2023) 584 - 603

CONTROL OF ELBOW REHABILITATION SYSTEM BASED ON OPTIMAL-TUNED BACKSTEPPING SLIDING MODE CONTROLLER

ZAHRAA A. WAHEED[1], AMJAD J. HUMAIDI[1,*], MUSAAB E. SADIQ[2], ARIF A. AL-QASSAR[1], ALAQ F. HASAN[3], AYAD Q. AL-DUJAILI[4], AHMED R. AJEL[4], SAAD J. ABBAS[5]

[1]Control and Systems Engineering Department, University of Technology, Baghdad, Iraq
[2]General Company for Grain Processing, Iraq
[3]Technical Engineering College, Middle Technical University, Baghdad, Iraq
[4]Middle Technical University, Electrical Engineering Technical College, Baghdad, Iraq
[5]AL Rafidain University College, Baghdad, Iraq
*Corresponding Author: amjad.j.humaidi@uotechnology.edu.iq

Abstract

The high nonlinearity and time-varying coefficients characterize the elbow exoskeleton system for rehabilitation. To deal with these difficult control challenges, nonlinear and reliable controllers are needed. This paper shows the use of Sliding Mode Control (SMC) and Backstepping Sliding Mode Control (BSMC) for trajectory tracking of an Elbow Exoskeleton System (EES) subjected to uncertainty in parameters. The Lyapunov stability analysis has been conducted to establish the control laws for the controlled elbow exoskeleton system based on SMC and BSMC. The Particle Swarm Optimization (PSO) algorithm is used to tuning the design parameters of suggested controllers for performance improvement. Computer simulation based on MATLAB software has been implemented to conduct a comparison study between the proposed controllers. The simulation findings showed that the optimal BSMC outperforms the optimal SMC in terms of tracking performance and robustness characteristics. In addition an improvement in performance of SMC and BSMC has been achieved when their design parameters are tuned based on PSO algorithm.

Keywords: Backstepping sliding mode control, Exoskeleton system, Rehabilitation.

1. Introduction

Due to a variety of circumstances, joint dysfunction disables a vast number of people each year. Control ability of muscle manifests itself in these people as torque production and a failure to modulate mechanical impedance around the joints [1-4]. Therefore, the rehabilitation procedures can be utilized by many of these disable patients to help them in restoring their health and returning to their regular life [5]. The accidents and pathology are the main cause of elbow disabilities in human being. In any of these circumstances, the resulting consequence leads to injury of muscles or nerve. This in turn leads to faults in motor functions and finally to paralysis. To provide a solution to problems in weakness of muscle and nerve, the assistive and rehabilitation equipment and tools came out to help the mobility of disabled individuals with various disabilities. In the Neuro-rehabilitation process, the programs have gradually been incorporated with aid of robotic devices [6].

Exoskeletons are wearable robots which are fit and interact with patient on a cognitive and physical system. These robotic exoskeleton systems work in conjunction with human limbs. Researches and developments of Exoskeleton devices have started in the early 1960s; however, they have been only recently applied in patients with motor deficits for functional replacement and rehabilitation. Theses exoskeleton devices are articulated mechanical systems which are supplied by sensors and actuators to achieve their functions properly. According to the size and weight of disables parts of human being, the types of actuators are dedicated that can achieve the stroke and force requirements of worn exoskeletal/orthotic system . In addition, the number of actuators depend on the number of joints to be exercised. In addition, the challenges of computation and control design are based on the number of degrees of freedoms (DoF) which are possessed by human musculoskeletal systems. As a result, if an efficient design is to be achieved, the control system is important. In order for the system to work properly, it needs to take into account factors like how quickly and where each limb moves, how well it can adapt to its environment, and how much energy each limb needs. These are all factors that must be taken into account [7-10].

Therefore, the need of robust control is an essential to develop successful control model for exoskeleton systems. In this study, two control strategies have been used for elbow exoskeleton system, namely: SMC and BSMC. It has been shown that the Sliding mode control technique is efficient in control of complex and higher order nonlinear systems in the presence of uncertainties. The SMC and BSMC are two ways to control things in a lot of different projects [11-16].

However, different control researches which are dedicated for motion control of human upper-limb are abbreviated in what follows: Barbouch et al. [17] have investigated the performance and robustness of a Feedback Error learning scheme mixed with sliding mode control (SMC) to motion control of elbow joint based on Functional Electrical Stimulation system]. Babaiasl et al. [18] presented new mechanical design of 3 DoF exoskeleton robot for rehabilitation of shoulder joint. The study proposed SMC to track desired trajectories and the genetic algorithm has been applied for optimal tuning of design parameters of proposed controller.

Nguyen et al. [19] developed adaptive intelligent controller which combines both fuzzy logic (FL) technique and PID control for upper-limb exoskeleton robot actuated by pneumatic artificial muscle. The PID controller is used to compensate the approximating error and hysteresis characteristics, while the FL part is

responsible for estimating the nonlinear functions. Hu et al. [20] have developed an assist-as-needed control algorithm for flexible exoskeletons applied for rehabilitation of upper-limb part of disabled patients. The elbow exoskeleton is mechanically designed to be driven by flexible antagonistic cable actuators.

Brahim et al. [21] presented backstepping sliding mode control design for pre-described path tracking of ETS-MARSE exoskeleton robot applied for passive rehabilitation exercises. The robot is worn by persons at the upper limb to help treatment of impaired upper limb functions due to stroke. Liu et al. [22] established adaptive fuzzy neural network (AFNN) for estimating the angle of elbow joint based on surface electromyography (sEMG). The AFNN showed better accuracy and rapidity as compared with other neural network structures, back-propagation-based NN and Radial basis-based NN.

Yang et al. [23] developed model free backstepping sliding mode control strategy for wearable exoskeletons. The non-singular fast terminal sliding controller is combined with auxiliary backstepping controller to improve the control performance. The lumped uncertainties are estimated via time-delay estimation. Bembli et al. [24] presented robust adaptive sliding mode algorithm based on gravity compensation to control the upper limb exoskeleton system subjected to parametric uncertainties. The rehabilitation system is two degrees of freedom robot to achieve movement of the elbow and shoulder joints.

Islam et al. [25] proposed fractional sliding mode control (FSMC) to control 7 DOF u-Rob (upper limb robotic exoskeleton) subjected to unmodeled dynamics. As compared to classical sliding mode control (SMC), the FSMC showed better performance in terms of tracking and chattering effect in control signal. Kiguchi et al. [26] proposed controller based on force sensor and electromyogram (EMG) signal of muscles to assist in motion of 3 DOF upper-limb for persons who are physically injured, disabled and elderly. The proposed controller took into account the force vector at the end-effector part in order to generate smooth and natural hand trajectories. In addition, the controlled upper-limb system involved obstacle avoidance algorithm to preventing the elements of upper-limb exoskeleton to collide with surrounding objects.

Kong et al. [27] presented the control design to realize virtual softness and flexibility of rigid-joint exoskeleton system without the ness of physical and real elastic devices. The proposed controlled has been developed based on normal distribution function and applied to five degree of freedom (5-DOF) rehabilitation exoskeleton. The stability has been proven for controlled system utilizing Riemann metric convergence analysis method and scalar energy function gradient method. Cui et al. [28] used ADRC (Active disturbance rejection control) to enhance the tracking performance in angular position of robot joints. The rehabilitation robot is actuated by multifilament muscles to represents the elbow-joint model and robot motion control. The proposed controller together with PID controller could quickly reject the disturbance signals without overshoot. The study conducted experimental passive rehabilitation training to verify the feasibility and effectiveness of ADRC and to ensure rationality, comfort safety and robustness of mechanical design.

Rahman et al. [29] focused on modelling and control for 2DOF Exoskeleton robot (ExoRob) for rehabilitating flexion/extension of elbow joint and internal/external rotation of shoulder joint. The proposed controller is designed

based on computed torque control (CTC) and a novel sliding mode control (SMC) using exponential reaching law.

In this study two control schemes, represented by SMC and BSMC, are designed to control the motion of elbow joint for exoskeleton rehabilitation system. The main contributions of this study can be highlighted by the following points:

- Development the control laws based of SLM and BSMC to guide the error trajectories from initial conditions to the zero equilibrium points.
- Conducting the stability analysis of both control schemes using Lyapunov-based stability analysis taking into account the uncertainties inherited in the elbow exoskeleton system.
- Design PSO algorithm for tuning the design parameters of elbow exoskeleton system to enhance the dynamic performance of controlled system.
- Reduce the chattering effect due to classical SMC by hybridization SMC with backing control methodology.

2. Modelling of Elbow Exoskeleton System

Figure 1 represents the exoskeleton device attached to the elbow. The device is used to assist motion of patient joint using actuator [25].

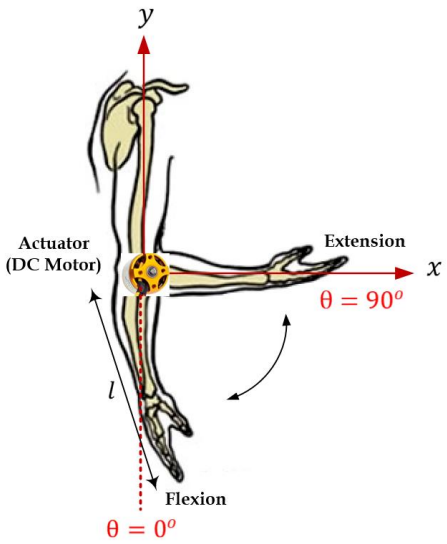

Fig. 1. Motion illustration for the flexion and extension in elbow.

The dynamic model of both human arm and exoskeleton are derived simultaneously. Euler-Lagrange equation is firstly established based on the following:

$$L_i = E_{ki} - E_{gi} \tag{1}$$

$$\frac{d}{dt}\frac{\partial L}{\partial \dot{\theta}} - \frac{\partial L}{\partial \theta} = \tau \tag{2}$$

where E_{ki} and E_{gi} are represented the kinetic and gravitational energies of the system and it is given by

$$E_{ki} = \frac{1}{2} I_i \dot{\theta}^2 \quad (3)$$

$$E_{gi} = g m_i l_i (1 - \cos\theta) \quad (4)$$

where I_i is the inertia of the human elbow and exoskeleton and $i\epsilon$ (1, 2), m_i , g and l_i represent the mass of the human elbow and exoskeleton, the acceleration due to gravity and the distance between the elbow joint and center of gravity, respectively [30].

$$I_i = \frac{1}{2} m_i l^2 \quad (5)$$

Substitution Eqs. (3) and (4) into Eq. (1) gives

$$L_i = \frac{1}{2} I \dot{\theta}^2 - g m_i l_i (1 - \cos\theta) \quad (6)$$

$$\tau_g = g\ m_i l_i \quad (7)$$

$$\tau_{exti} = \tau_{fi} + \tau_i \quad (8)$$

where τ_g and τ_{exti} represent the system's gravitational torque and external torque acting on the system, and τ_{fi} and τ_i represent the friction and motor control torque respectively.

$$\tau_{fi} = k_v \dot{\theta} \quad (9)$$

where k_v represent viscous friction coefficients

On deriving Eq. (6), using Euler-Lagrange equation the resulting dynamics of the system can be written as:

$$\tau_e = I\ddot{\theta} - \tau_g \sin\theta \quad (10)$$

Let $\tau_i = \tau_e$, which is the single applied torque, then Eq. (11) becomes

$$\tau_i = I\ddot{\theta} - \tau_g \sin\theta \quad (11)$$

The system model consists of the human leg and exoskeleton is given by

$$I\ddot{\theta} = \tau_g \sin\theta - k_v\dot{\theta} + \tau_e \quad (12)$$

where, $I = \sum_{i=1}^{2} I_i$, $F = \sum_{i=1}^{2} F_i$ $B = \sum_{i=1}^{2} B_i$ $\theta, \dot{\theta}, \ddot{\theta}$ represent the angular position, velocity, and acceleration of the coupled system respectively. Equation (12) can be written robotic form as follows:

$$M(\theta)\ \ddot{\theta} + f\left(\theta, \dot{\theta}\right) + G(\theta) = \tau_e \quad (13)$$

Hence, Eq. (13) can be written as:

$$\ddot{\theta} = M(\theta)^{-1}\left(\tau_e - f\left(\theta, \dot{\theta}\right) - G(\theta)\right) \quad (14)$$

In addition, Eq. (14) can be written in state variables as follows:

$$\dot{x}_1 = \dot{\theta} = x_2 \quad (15)$$

$$\dot{x}_2 = \ddot{\theta} = \frac{1}{I}(\tau_e - k_v x_2 + \tau_e\, sin(x_1)) \quad (16)$$

3. Design of SMC and BSMC for Elbow Elbow-Exoskeleton System

In this part, the control laws are developed based on SMC and BSMC in the presence of uncertainty in system parameters. The sliding surface is synthesized to derive the control law based on controlled system. However, two assumptions have to be followed for developing the control laws of SMC and BSMC [31-37]:

Assumption 1: The dynamic model of coupled human-exoskeleton system has been described by Eqs. (15) and (16) without taking the dynamic of DC motor. This assumption is reasonable if the time response of motor is fast enough.

Assumption 2: The elbow movement has been limited with the angular span indicated in Fig. 1.

3.1. SMC design for elbow-exoskeleton system

If error e is assigned to the difference between the current position $x_1 = \theta$ and the desired trajectory $x_{1\mathrm{d}}=\theta_{\mathrm{d}}$,

$$e = x_1 - x_{1d} \tag{17}$$

Using Eqs. (15) and (16), the first and second derivative is given by Humaidi et al. [31]:

$$\dot{e} = \dot{x}_1 - \dot{x}_{1d} = x_2 - \dot{x}_{1d} \tag{18}$$

$$\ddot{e} = \dot{x}_2 - \ddot{x}_{1d} \tag{19}$$

$$\ddot{e} = \frac{1}{I}\left(\tau_e - K_v\, x_2 + \tau_g \sin(x_1)\right) - \ddot{x}_{1d} \tag{20}$$

where, τ represent the applied torque or the actuating control signal. The sliding surface is chosen according to the order of controlled system:

$$s = c\, e + \dot{e} \tag{21}$$

Using Eqs. (18) and (20), the first-time derivative of sliding surface equation is given by

$$\dot{s} = c\, \dot{e} + \dot{x}_2 - \ddot{x}_{1d} \tag{22}$$

where, c is defined as scalar design parameter. According to Eq. (16), Eq. (22) becomes

$$\dot{s} = c\, \dot{e} + \frac{1}{\mathrm{I}}\left(\tau_{\mathrm{e}} - K_v\, x_2 + \tau_g \sin(x_1)\right) \text{-} \ddot{x}_{1d} \tag{23}$$

Letting $\tau_e = u$, Eq. (23) can be written as

$$\dot{s} = c\, \dot{e} + \frac{1}{\mathrm{I}}\left(\mathrm{u} - K_v\, x_2 + \tau_g \sin(x_1)\right) \text{-} \ddot{x}_{1\mathrm{d}} \tag{24}$$

Based on SMC approach, the control law u is composed of

$$u = u_{eq} + u_{sw} \tag{15}$$

where u_{eq} is the equivalent part and u_{sw} represents the switching part; that is,

$$u_{eq} = I.\left(K_v\, x_2 - \tau_g \sin(x_1)\right) - c\, \dot{e} + \ddot{x}_{1d} \tag{26}$$

$$u_{sw} = \text{-}\beta_1 sign\,(s) \tag{27}$$

where, β_1 represents a scalar design constant. When setting sliding surface and its derivative to zero ($s = 0$, $\dot{s} = 0$), The control law u can be deduced

$$u = \mathrm{I}.\,(K_v\, x_2 - \tau_e \sin(x_1)) - c\, \dot{\mathrm{e}} + \ddot{x}_{1d} - \beta_1 \mathrm{sign(s)} \tag{28}$$

3.2. BSMC design for elbow-exoskeleton system

The critical issue with SMC is the presence of chattering problem in control signal due to sign function. The development of BSMC can solve this problem and it can considerably reduce the chattering effect. Moreover, the BSMC can reduce the

effect of uncertainties in the parameters of elbow exoskeleton system. The algorithmic design of BSMC can be developed based on the following steps:

Step 1:

The tracking error and its derivative is given respectively as [32]:

$$e_1 = x_{1d} - x_1 \tag{29}$$

$$\dot{e}_1 = \dot{x}_{1d} - \dot{x}_1 = \dot{x}_{1d} - x_2 \tag{30}$$

The first choice of Lyapunov Function (L.F.) is given by:

$$V_1 = \frac{1}{2} e_1^2 \tag{31}$$

Substituting Eq.(29) into the time derivative of L.F. gives

$$\dot{V}_1 = e_1 \dot{e}_1 = e_1 \, (\dot{x}_{1d} - x_2) \tag{32}$$

Letting α_1 to be the virtual control and equal to x_2; that is,

$$x_2 = \alpha_1 = \dot{x}_{1d} + c_1' \, e_1 \tag{33}$$

where c_1' is a positive constant. Using Eqs. (32) and (33) becomes

$$\dot{V}_1 = -c_1' \, e_1^2 \leq 0 \tag{34}$$

Step 2:

Let e_2 represent the error between virtual control and desired control [32]:

$$e_2 = x_2 - \alpha_1 = x_2 - \dot{x}_{1d} - c_1' \, e_1 \tag{35}$$

The time derivative of e_2 is given by

$$\dot{e}_2 = \ddot{x}_1 - \dot{\alpha}_1 = \dot{x}_2 - \dot{\alpha}_1 \tag{36}$$

Based on Eq. (35), the time derivative of virtual control $\dot{\alpha}_1$ is given by

$$\dot{\alpha}_1 = \ddot{x}_{1d} + c_1' \, \dot{e}_1 \tag{37}$$

According to Eq. (36) and Eq. (16), Eq. (35) becomes

$$\dot{e}_2 = \frac{1}{\mathrm{I}} \left(\mathrm{u} - K_v \, x_2 + \tau_g \sin(x_1) \right) - \ddot{x}_{1\mathrm{d}} - c_1' \, \dot{e}_1 \tag{38}$$

The second candidate of L.F. and its time derivative are, respectively, given by

$$V_2 = \frac{1}{2} e_1^2 + \frac{1}{2} e_2^2 \tag{39}$$

$$\dot{V}_2 = e_1 \, \dot{e}_1 + e_2 \, \dot{e}_2 \tag{40}$$

Using Eq. (30), one can obtain

$$\dot{V}_2 = e_1 (\dot{x}_{1d} - x_2) + \, e_2 \, \dot{e}_2 \tag{41}$$

From Eq. (35), one can have

$$x_2 = e_2 + \alpha_1 = e_2 + \dot{x}_{1d} + c_1' e_1 \tag{42}$$

$$\dot{V}_2 = e_1 \, (\dot{x}_{1d} - e_2 - \dot{x}_{1d} - c_1' \, e_1) + e_2 \left(\frac{1}{I} \left(\mathrm{u} - K_v \, x_2 + \tau_g \sin(x_1) \right) - \ddot{x}_{1\mathrm{d}} - c_1' \, \dot{e}_1 \right)$$

or,

$$\dot{V}_2 = -c_1' \, e_1^2 - e_1 \, e_2 \, + e_2 \left(\frac{1}{I} \left(\mathrm{u} - K_v \, x_2 + \tau_g \sin(x_1) \right) - \ddot{x}_{1\mathrm{d}} - c_1' \, \dot{e}_1 \right) \tag{43}$$

In order to ensure $\dot{V}_2 < 0$, the control u has to be chosen as follow

$$u = K_v \, x_2 - \tau_g \sin(x_1) + I \, \ddot{x}_{1\mathrm{d}} + I \, c_1' \, \dot{e}_1 - I \, c_2' \, e_2 + I \, e_1 \, e_2 \tag{44}$$

Therefore, Eq. (43) becomes

$$\dot{V}_2 = -c_1' e_1^2 - c_2' e_2^2 \leq 0 \quad (45)$$

where, c_2 represents positive constant of real value. According to Eq. (45), one can deduce that the developed control law can ensure negative definite of $\dot{V}_2$ and hence the asymptotic stability of controlled system can be proven.

Step 3:

The sliding surface can be defined in terms of tracking errors [32]:

$$s = e_2 + c_3' e_1 \quad (46)$$

Substituting Eq. (34) into Eq. (46) to have

$$s = x_2 - \dot{x}_{1d} - c_1' e_1 + c_3' e_1 \quad (47)$$

The time derivative of sliding surface is given by

$$\dot{s} = \dot{x}_2 - \ddot{x}_{1d} - c_1'\dot{e}_1 + c_3 \dot{e}_1 \quad (48)$$

Equation (48) can be rewritten as

$$\dot{s} = \dot{x}_2 - \ddot{x}_{1d} - c_4'\dot{e}_1 \quad (49)$$

where, $c_4' = (c_1' - c_3')$ is a positive real constant. Applying Eq. (16) and (49) can be given by

$$\dot{s} = \frac{1}{I}\left(\mathrm{u} - K_v x_2 + \tau_g \sin(x_1)\right) - \ddot{x}_{1d} - c_4'\dot{e}_1 \quad (50)$$

The L.F. is defined taking into account the sliding surface:

$$V_2 = \frac{1}{2}e_1^2 + \frac{1}{2}s^2 \quad (51)$$

If the time derivative of Eq. (51) is taken and using Eqs. (30) and (50), one can obtain

$$\dot{V}_2 = e_1 \dot{e}_1 + s\left(\frac{1}{I}\left(\mathrm{u} - K_v x_2 + \tau_g \sin(x_1)\right) - \ddot{x}_{1d} - c_4'\dot{e}_1\right) \quad (52)$$

Using Eq.(47) and Eq.(30) to have

$$\dot{e}_1 = -s - c_4' e_1 \quad (53)$$

Substituting Eq. (53) into Eq. (52) to get

$$\dot{V}_2 = e_1(-s - c_4' e_1) + s\left(\frac{1}{I}\left(\mathrm{u} - K_v x_2 + \tau_g \sin(x_1)\right) - \ddot{x}_{1d} - c_4'\dot{e}_1\right)$$

or,

$$\dot{V}_2 = -c_4' e_1^2 + s\left(-e_1 + \frac{1}{I}\left(u - k_v x_2 + \tau_g sin(x_1)\right) - \ddot{x}_{1d} - c_4' \dot{e}_1\right) \quad (54)$$

To ensure $\dot{V}_2 \leq 0$, the control law has to be chosen as follows

$$u = k_v x_2 + \tau_g sin(x_1) + I \ddot{x}_{1d} + I c_4' \dot{e}_1 + I e_1 - c_5' s \quad (55)$$

The control law described by Eq. (55) represents the equivalent part of control signal. The switching part of control signal is given by

$$u_{sw} = -\beta_2' sign(s) \quad (56)$$

where, β_2' is a scalar design gain The overall control signal consists of the equivalent and switching parts; i.e.,

$$u = k_v x_2 + \tau_g sin(x_1) + I \ddot{x}_{1d} + I c_4' \dot{e}_1 + I e_1 - c_5' s \quad (57)$$

Taking into account the equivalent control part of BSMC, Eq. (54) becomes

$$\dot{V}_2 = -c_4' e_1^2 - c_5' s^2 - \beta_2' |s| \leq 0 \quad (58)$$

Since $\dot{V}_2$ is negative definite, then based on the Lyapunov theorem, the system's trajectories will be attracted towards the sliding surface and remain sliding on it until they reach the origin in asymptotic manner. The design parameters stated above should be chosen such that $\dot{V}_2 < 0$ has to be satisfied at all times.
Other control strategies can be suggested and designed to control the motion of elbow part and a comparison study can be conducted between the proposed controller and these suggested controller [38-46].

4. Parameters Optimization

The BSMC controllers' design parameters need to be adjusted to get the best controller performance from SMC controllers for the Elbow-Exoskeleton system. The trial-and-error method of determining or adjusting these parameters is inefficient and does not produce the best results in terms of improved dynamic performance of controlled systems. As a result, the PSO technique has been suggested as a means of determining the optimal values of these parameters in order to achieve perfect performance of the proposed controllers in terms of dynamic responsiveness. The design parameters for SMC are (c, β_1), but for BSMC, they are (c_1, c_3, c_5).

PSO particles modify their velocity to traverse throughout the search (solution) space depending on their own and other particles' search experiences. Based on how many times it has been performed, each particle must update its velocity and location. Of course, this job will be done based on a cost function in order to minimize or maximize the cost. In our design, we have to keep the cost function as low as possible [47-51].

The velocity of each particle changes as shown in the Eq. (59) below:

$$V_i^{k+1} = wV_i^k + C_1 \text{rand}\left(p_{best} - X_i^k\right) + C_2 \text{rand}\left(g_{best} - X_i^k\right) \quad (59)$$

where w is the inertia coefficient, C_1 denotes the personal acceleration coefficient, and C_2 denotes the societal acceleration coefficient The following equation changes each particle's position:

$$X_i^{k+1} = X_i^k + V_i^{k+1} X_i^k \quad (60)$$

where X_i^{k+1} indicates the current and updated vectors, respectively. Throughout the search for the lowest Root Mean Square Error (RMSE), the RMSE function is chosen as the cost function for evaluating each particle. The parameters for PSO algorithms employed in this investigation are listed in Table 1.

Table 1. Test model specifications and test conditions.

PSO Algorithm Parameters	Value
W (inertia coefficient)	1.4
Personal acceleration coefficient C1	2
Social acceleration coefficient C2	2
Population size	20
Iterations No.	300

In the literature, there are different modern optimization techniques can be pursued for optimal tuning of design parameters such as Wale Optimization Algorithm (WOA), Social Spider Optimization (SSO), Grey-Wolf Optimization (GWO), butterfly optimization algorithm (BOA), chicken swarm optimization (CSO), and Spider Monkey Optimization (SMO) [52-58]. The results due to the suggested optimization methods can be used as a comparison study with that based on proposed PSO algorithm.

5. Computer Simulation of Elbow-Exoskeleton System Controlled by SMC and BSMC

Table 2 lists the numerical values for the Elbow-Exoskeleton system case. The MATLAB software was used to model all of the proposed controllers as well as the entire system. The simulation results were running for 3 seconds.

Table 2. Test model specifications and test conditions.

Coefficient Description	Value
Mass M	1.55 kg
Length l	0.24 m
Elbow joint to centre of gravity is l l_i	0.2 m
Gravity Acceleration g	9.81m/s^2
viscous friction coefficients k_v	1.5 Nm/(rad/s)

Figure 2 shows the open-loop test of Elbow-Exoskeleton system. The system is commanded by sine wave method. It is clear from the figure that the output response, represented by linear displacement x_1, has started from high position (1.6) rad, however, the response settles quickly just after around (2) seconds to reach nearly zero rad. The c and β_1 are the design parameters of SMC, while for BSMC, c_1, c_3, c_5 and β_2 are the designs parameters.

However, the setup values differ from those based on SMC. For BSMC, the parameter design gain β_2 is considered to be 1000. Increasing the dynamic performance of SMC and BSMC by optimizing their design parameters is an objective of the PSO algorithm. As with other PSO processes, the iterative particles are evaluated using the RMSE fitness function.

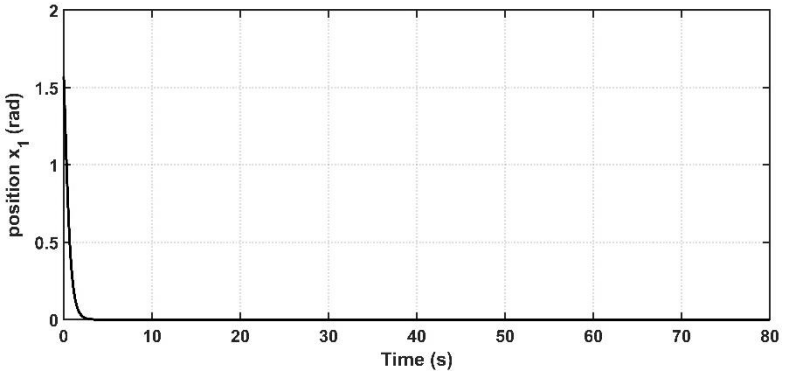

Fig. 2. Open loop response for the elbow-exoskeleton system.

The goal of an optimization technique is to identify the best values for design parameters such that the RMSE is as low as possible. Figures 3 and 4 show the behaviour of the cost function for SMC and BSMC a respectively. From the aforementioned Figs. 3 and 4, the superiority of BSMC is obvious in terms of cost reduction.

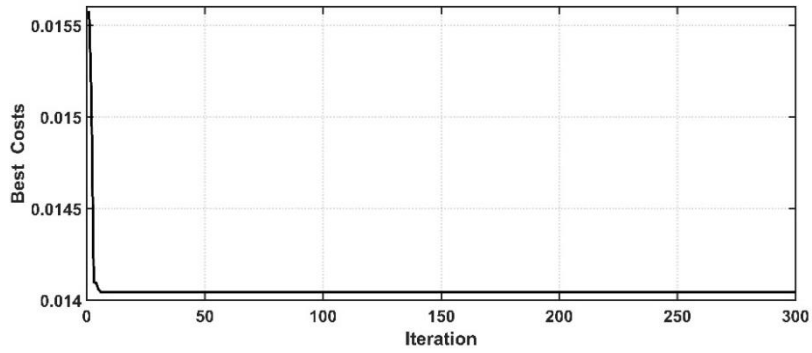

Fig. 3. Cost function for controlled system based on SMC.

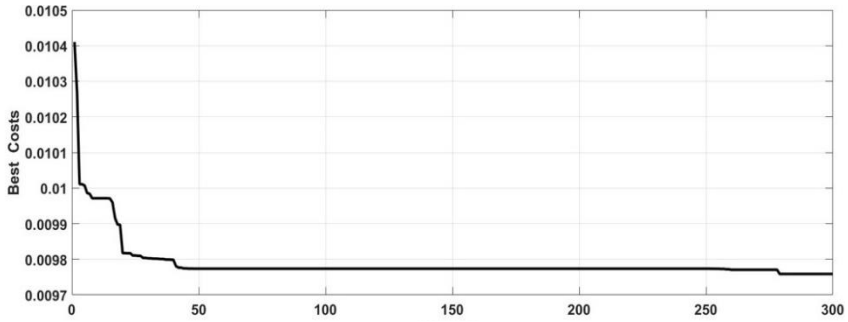

Fig. 4. BSMC-based cost function for controlled system.

Table 3 gives the two settings of design parameters Elbow-Exoskeleton System by SMC and BSMC. The PSO algorithm was used to find the first set of design parameters, while the trial-and-error method was used to determine the second set. In order to provide the best possible control of the system, the optimum values of the design parameters determined via the PSO technique are transferred to the controllers' corresponding design parameters. The expected trajectory assumes a sine wave input.

Table 3. Setting of design parameters for different controllers of elbow-exoskeleton system.

Controller	Optimal Values		Try and Error Values	
	Coefficient	**Value**	**Coefficient**	**Value**
SMC	c	54.7070	c	39.3654
	β_1	561.14246	β_1	255
BSMC	c_1'	159.9826	c_1'	150
	c_3'	20.1799	c_3'	20
	c_5'	1.0398×10^3	c_5'	900

Elbow-exoskeleton actuated system based on SMC and BSMC

Figure 5 shows the linear position behaviour of the Elbow-Exoskeleton-actuated based on the optimal SMC and BSMC to obtain the tracking performance for the system. The figure reflects the fact that the tracking error (e_1) based on BSMC is less than that due to SMC, and thus BSMC gives better dynamic performance.

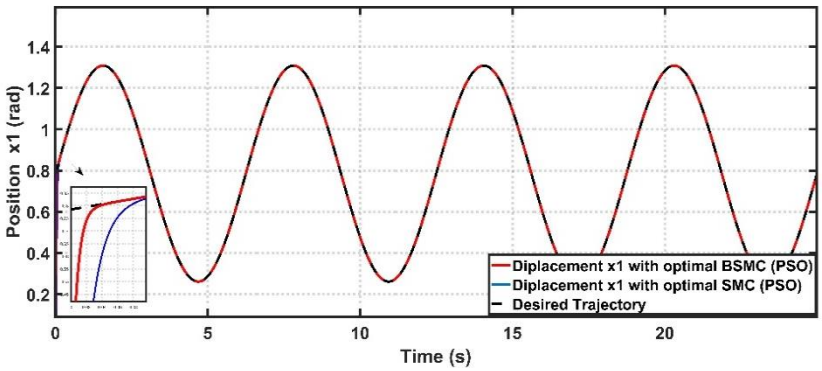

Fig. 5. Track the performance of the SMC and BSMC elbow-exoskeleton system actuated systems.

Figure 6 illustrates the behaviours of tracking errors due to optimal SMC and BSMC. It is worth to mention that we have simulated optimized SMC and BSMC parameters in which their error was 0.0097 and 0.014 respectively compared with 0.0215 and 0.0105 for non-optimized SMC and BSMC respectively. However, it is clear that BSMC over perform SMC. Figure 7 shows the derivative of tracking error.

Figure 8 depicts the SMC and BMC sliding surfaces, as well as the trace of the path in phase plane coordinates ($e - \dot{e}$). According to the figure, the trajectory starts at initial states on the e-axis and the equivalent control part is responsible for transferring the trajectory from initial condition to sliding surface. Upon reaching the sliding surface, the switching part of control signal undertakes the trajectory along the sliding surface to the equilibrium points. The conclusion drawn by this plot is that the designed controller could takes the trajectory from initial condition to equilibrium point via sliding surface.

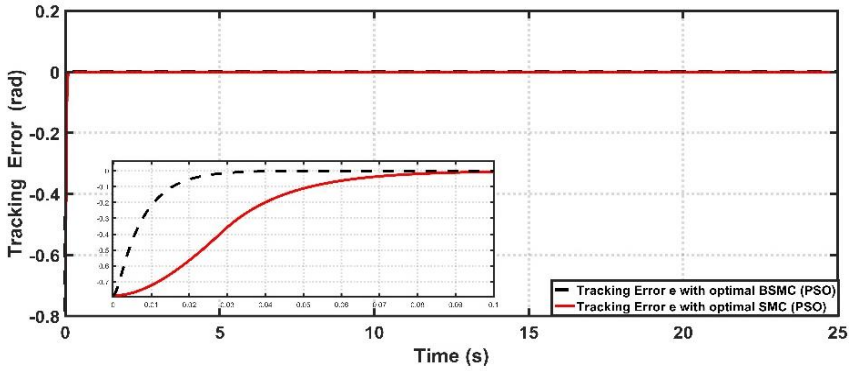

Fig. 6. Tracking error of SMC and BSMC controlled elbow-exoskeleton system.

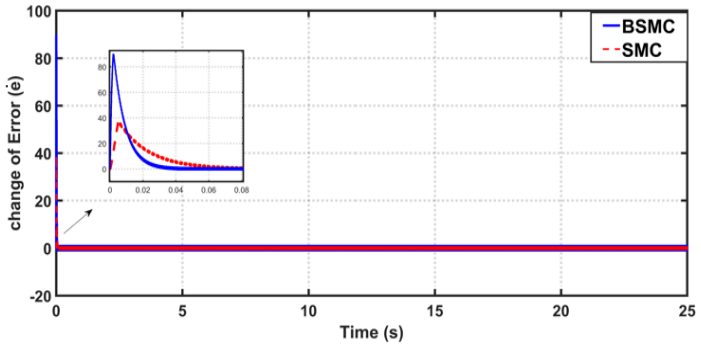

Fig.7. Change of tracking error for controlled elbow-exoskeleton system based on SMC and BSMC.

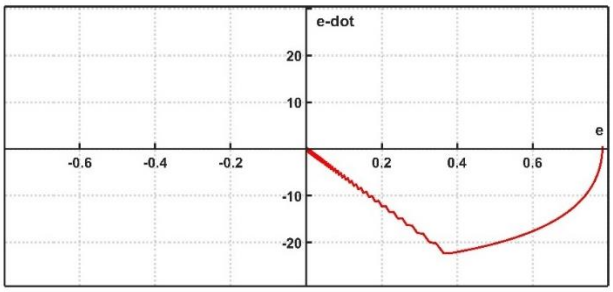

Fig. 8. Sliding surface of SMC.

The effect of chattering phenomenon due to the SMC and BSMC is illustrated Fig. 9. According to Fig. 8, it evident from the response of angular position that the chattering effect is due to the SMC, while this the chattering behaviour has disappeared at the response under BSMC. In other words, the BSMC could considerably reduce the effect of chattering resulting from SMC. Figure 10 exhibits the corresponding control signals generated by both SMC and BSMC for actuating the elbow-exoskeleton devices. This figure indicates that the BSMC has less control effort than that exerted by SMC. In addition, the chattering behaviour in the control effort due to SMC is higher than BSMC. This indicates that the BSMC has better chattering rejection capability, in both position response and control signal, as compared to SMC.

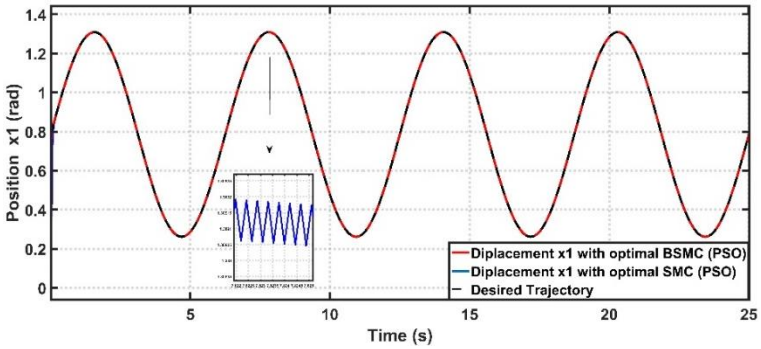

Fig. 9. Chattering phenomenon based on SMC and BSMC.

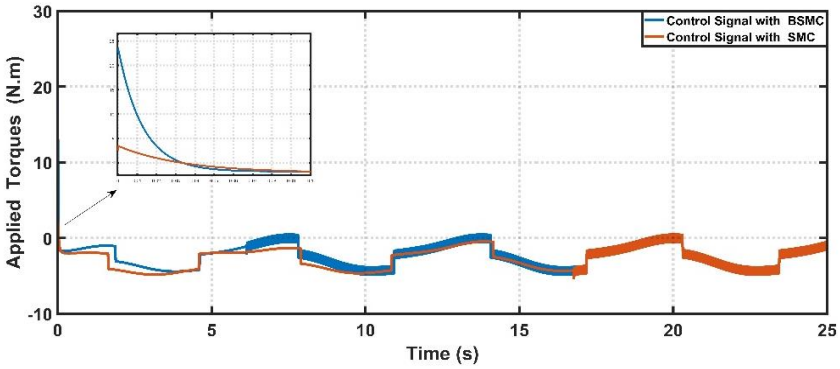

Fig. 10. Control effects based on SMC and BSMC.

In Fig. 11, the robustness of proposed controller has been tested against variation in system parameters. The mass of patient's arm has been increased by 20% at time 10 s. The figure shows that the BSMC has better robustness characteristics than SMC under variation of system parameters.

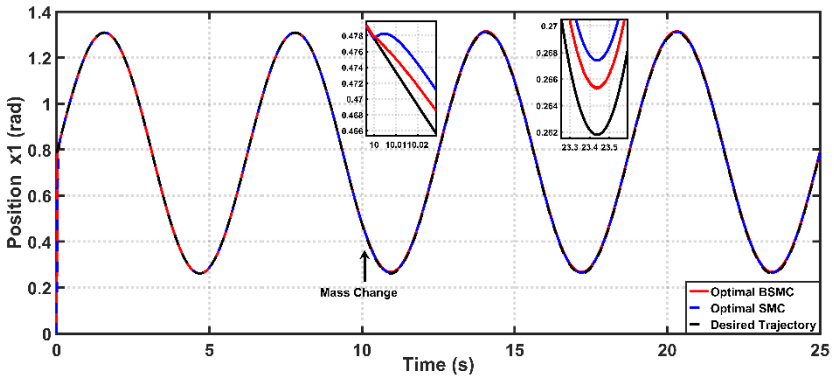

Fig. 11. Robustness characteristics of BSMC and SMC against variation of system mass

This study can be extended by implementing the proposed controller in real-time environment. Either Arduino microcontroller, single-board computer like Raspberry-Pi, or other semiconductor devices like Field Programming Gate Array (FPGA) can be used to synthesize the proposed controller [59-62].

6. Conclusions

In this study, two control schemes have been designed for trajectory control tracking of elbow-assistive rehabilitation system. The first control approach is based on sliding mode control, while the other control approach is developed based on backstepping sliding mode control methodology. The numerical results have showed that the performance of BSMC outperforms the SMC in terms of tracking error and robustness characteristics against variation in parameters elbow-exoskeleton system. In addition, the BSMC has better chattering rejection capability in both position response and control signal as compared to SMC. The other contribution of the

present work focused on the effect of PSO algorithm to tune the design parameters of SMC and BSMC. The results showed that PSO tuner could considerably enhanced the dynamic performance of proposed controllers.

Nomenclatures

C_1	Personal acceleration coefficient
C_2	Social acceleration coefficient
c	Scalar design
e	Difference between the current position desired trajectory
E_{ki}	Kinetic energies
Eg_i	Gravitational energies
l	Length
Li	Euler-Lagrange
l_i	Elbow joint to centre of gravity
$\mathcal{g}$	Gravity Acceleration
Mi	Mass of the human elbow and exoskeleton
k_v	Viscous friction coefficients
s	Sliding surface
$\mathcal{W}$	Inertia coefficient
X_{1d}	Desired trajectory

Greek Symbols

α_1	Virtual control
β_1	Scalar design constant.
β_2'	scalar design gain
θ	Angular position
$\dot{\theta}$	Angular velocity
$\ddot{\theta}$	Angular acceleration
τ_{exti}	External torque
τ_{fi}	Friction control torque
τ_g	Gravitational torque
τ_i	Motor control torque

Abbreviations

AFNN	Adaptive Fuzzy Neural Network
BSMC	Backstepping Sliding Mode Control
Dof	Degrees of freedoms
EES	Elbow Exoskeleton System
FL	Fuzzy Logic
FSMC	fractional sliding mode control
RMSE	Root Mean Square Error
SMC	Sliding Mode Control

References

1. Mahdi, S.M.; Yousif, N.Q.; Oglah, A.A.; Sadiq, M.E.; Humaidi, A.J.; and Azar, A.T. (2022). Adaptive synergetic motion control for wearable knee-assistive system: A rehabilitation of disabled patients. *Actuators*, 11(7), 176.

2. Waheed, Z.A.; and Humaidi, A.J. (2022). Design of optimal sliding mode control of elbow wearable exoskeleton system based on whale optimization algorithm. *Journal Européen des Systèmes Automatisés*, 55(4), 459-466.
3. Alawad, N.A.; Humaidi, A.J.; and Alaraji, A.S. (2022). Fractional proportional derivative-based active disturbance rejection control of knee exoskeleton device for rehabilitation care. *Indonesian Journal of Electrical Engineering and Computer Science*, 28(3), 1405-1413.
4. Salman, M.A.; and Kadhim, S.K. (2022). Optimal Backstepping Controller Design for Prosthetic Knee Joint. *Journal Européen des Systèmes Automatisés*, 55(1), 49-59.
5. Ahmed, N.; Humaidi, A.; and Sabah, A. (2022). Clinical trajectory control for lower knee rehabilitation using ADRC method. *Journal of Applied Research and Technology*, 20(5), 576-583.
6. Collinger, J.L.; Foldes, S.; Bruns, T.M.; Wodlinger, B.; Gaunt, R; and Weber, D.J. (2013). Neuroprosthetic technology for individuals with spinal cord injury. *Journal of Spinal cord Medicine*, 36(4), 258-272.
7. Herr, H. (2009). Exoskeletons and orthoses: classification, design challenges and future directions. *Journal of NeuroEngineering and Rehabilitation*, 6:21, 1-9.
8. Alawad, N.A.; Humaidi, A.J.; Al-Obaidi, A.S.M.; and Alaraji, A.S. (2022). Active disturbance rejection control of wearable lower-limb system based on reduced ESO. *Indonesian Journal of Science & Technology*, 7(2), 203-218.
9. Dollar, A.M.; and Herr, H. (2008). Lower extremity exoskeletons and active orthoses: challenges and state-of-the-art. *IEEE Transactions on Robotics*, 24(1), 144-158.
10. Alawad, N.A.; Humaidi, A.J.; and Al-Araji, A.S. (2022). Improved active disturbance rejection control for the knee joint motion model. *Mathematical Modelling of Engineering Problems*, 9(2), 477-483.
11. Falah, A.; Humaidi, A.J.; Al-Dujaili, A.; and Ibraheem, I.K. (2020). Robust super-twisting sliding control of PAM- actuated manipulator based on perturbation observer. *Cogent Engineering*, 7(1), 1858393.
12. Al-Dujaili, A.Q.; Falah, A.; Humaidi, A.J.; Pereira, D.A.; and Ibraheem, I.K. (2022). Optimal super-twisting sliding mode control design of robot manipulator: Design and comparison study. *International Journal of Advanced Robotic Systems*, 17(6), 1-17.
13. Adamiak, K. (2020). Chattering-free reference sliding variable-based SMC. *Mathematical Problems in Engineering*, Volume 2020, Article ID 3454090, 1-16.
14. Hussein, E.Q.; Al-Dujaili, A.Q.; and Ajel, A.R. (2020). Design of sliding mode control for overhead crane systems. *IOP Conference Series*: *Materials Science and Engineering*, 881, 012084.
15. Mohammed, A.K.; Al-Shamaa, N.K.; and Al-Dujaili, A.Q. (2022). Super-twisting sliding mode control of permanent magnet DC motor. *Proceedings of the* 2022 *IEEE* 18*th International Colloquium on Signal Processing & Applications* (*CSPA*), Selangor, Malaysia, 347-352.
16. Mohammed, A.M.; Al-Samarraie, S.A.; and Jaber, A.A. (2022). Design of a robust controller for a gearbox connected two-mass system based on a hybrid model. *FME Transactions*, 50(1), 79-89.

17. Barbouch, H.; Resquín, F.; Gonzalez-Vargas, J.; Hadded, N.K.; and Belghith, S. (2019). Feedback error learning with sliding mode control for functional electrical stimulation: Elbow joint simulation. *International Journal of Innovative Technology and Exploring Engineering*, 8(12), 2971-2982.
18. Babaiasl, M.; Goldar, S.N.; Barhaghtalab, M.H.; and Meigoli, V. (2015). Sliding mode control of an exoskeleton robot for use in upper-limb rehabilitation. *Proceedings of the* 2015 3*rd RSI International Conference on Robotics and Mechatronics* (*ICROM*), Iran, 694-701.
19. Nguyen, H.T.; Trinh, V.C.; and Le, T.D. (2020). An adaptive fast terminal sliding mode controller of exercise-assisted robotic arm for elbow joint rehabilitation featuring pneumatic artificial muscle actuator. *Actuators*, 9(4), 118, 1-14.
20. Hu, B.; Zhang, F.; Lu, H.; Zou, H.; Yang, J.; Yu, H. (2021). Design and assist-as-needed control of flexible elbow exoskeleton actuated by nonlinear series elastic cable driven mechanism. *Actuators*, 10(11), 290.
21. Brahim B.; Rahman M.H.; Saad M.; Luna C.O. (2016). Sliding mode-backstepping control for upper-limb rehabilitation with the ets-marse exoskeleton robot. *Conference in Promoting Access to Assistive Technology RESNA/NCART*, 1-7.
22. Liu, Y.; Li, C.; Teng, Z., Liu, K., Wang, G.; and Sun Z. (2020). Intention recognition of elbow joint based on sEMG using adaptive fuzzy neural network. *Proceedings of the* 2020 5*th International Conference on Mechanical, Control and Computer Engineering* (*ICMCCE*), Harbin, China, 1091-1096.
23. Yang, P.; Sun, J., Wang, J.; Zhang, G.; and Zhang, Y. (2019). Model-free based back-stepping sliding mode control for wearable exoskeletons. *Proceedings of the* 2019 25*th International Conference on Automation and Computing* (*ICAC*), Lancaster, UK, 1-6.
24. Bembli S.; Haddad N.K.; and Belghith S. (2019). Adaptive sliding mode control with gravity compensation: Application to an upper-limb exoskeleton system. MATEC Web of Conferences, Volume 261, 06001, 1-8.
25. Islam, M.R.; Rahmani, M.; and Rahman, M.H. (2020). A novel exoskeleton with fractional sliding mode control for upper limb rehabilitation. *Robotica*, 38(11), 2099-2120.
26. Kiguchi, K.; Rahman, M.H.; Sasaki, M.; and Teramoto, K. (2008). Development of a 3DOF mobile exoskeleton robot for human upper-limb motion assist. *Robotics and Autonomous Systems*, 56(8), 678-691.
27. Kong, D.; Wang, W.; Shi, Y.; and Kong, L. (2022). Flexible control strategy for upper-limb rehabilitation exoskeleton based on virtual spring damper hypothesis. *Actuators*, 11(5), 138.
28. Cui, X.; Wang, B.; Lu, H.; and Chen, J. (2021). Design and passive training control of elbow rehabilitation robot. *Electronics*, 10(10), 1147.
29. Rahman, M.H.; Ouimet, T.K.; Saad M.; Kenné, J.P.; and Archambault P.S. (2010). Development and control of a wearable robot for rehabilitation of elbow and shoulder joint movements. *Proceedings of IECON* 2010 - 36*th Annual Conference on IEEE Industrial Electronics Society*, Glendale, AZ, USA, 1506-1511.

30. Dinh, B.K.; Xiloyannis, M; Antuvan, C.W.; Cappello, L.; and Masia, L. (2017). Hierarchical cascade controller for assistance modulation in a soft wearable arm exoskeleton. *IEEE robotics and Automation Letters*, 2(3), 1786-1793.
31. Humaidi, A.J.; Hameed, M.R.; and Hameed, A.H. (2018). Design of block-backstepping controller to ball and arc system based on zero dynamic theory. *Journal of Engineering Science and Technology* (*JESTEC*), 13(7), 2084-2105.
32. Hassan, M.Y.; Humaidi, A.J.; and Hamza, M.K. (2020). On the design of backstepping controller for Acrobot system based on adaptive observer. *International Review of Electrical Engineering*, 15(4), 328-335.
33. Basri, M.A.M. (2018). Design and application of an adaptive backstepping sliding mode controller for a six-DOF quadrotor aerial robot. *Robotica*, 36(11), 1701-1727.
34. Humaidi, A.J.; and Hameed, M. (2019). Development of a new adaptive backstepping control design for a non-strict and under-actuated system based on a PSO tuner. *Information*, 10(2), 38, 1-17.
35. Humaidi, A.J.; Sadiq, M.E.; Abdulkareem, A.I.; Ibraheem, I.K.; and Azar, A.T. (2021). Adaptive backstepping sliding mode control design for vibration suppression of earth-quaked building supported by magneto-rheological damper. *Journal of Low Frequency Noise, Vibration and Active Control*, 41(2):768-783.
36. Humaidi, A.J.; and Hameed, M.R. (2017). Design and performance investigation of block-backstepping algorithms for ball and arc system. *Proceedings of the* 2017 *IEEE International Conference on Power, Control, Signals and Instrumentation Engineering* (*ICPCSI*). Chennai, India, 325-332.
37. Humaidi, A.J.; Talaat, E.N.; Hameed, M.R.; and Hameed, A.H. (2019). Design of adaptive observer-based backstepping control of cart-pole pendulum system. *Proceedings of the* 2019 *IEEE International Conference on Electrical, Computer and Communication Technologies* (*ICECCT*). Coimbatore, India, 1-5.
38. Kasim, M.Q.; and Hassan, R.F. (2021). Reduced computational burden model predictive current control of asymmetric stacked multi-level inverter based STATCOM. *Proceedings of the* 2021 *IEEE International Conference on Automatic Control & Intelligent Systems* (*I2CACIS*), Shah Alam, Malaysia, 374-379.
39. Humaidi, A.J.; and Hameed, A.H. (2017). Robustness enhancement of MRAC using modification techniques for speed control of three phase induction motor. *Journal of Electrical Systems*, 13(4), 723-741.
40. Jaber, A.A.; Ali, K.M. (2019). Artificial neural network based fault diagnosis of a pulley-belt rotating system. *International Journal on Advanced Science, Engineering and Information Technology*, 9(2), 544-551.
41. Al-Khazraji, H.; Nasser, A.R; Hasan, A.M.; Al Mhdawi A.K.; Al-Raweshidy, H.; and Humaidi, A.J. (2022). Aircraft engines remaining useful life prediction based on a hybrid model of autoencoder and deep belief network. *IEEE Access*, 10, 82156-82163.
42. Humaidi, A.J.; and Hussein, H.A. (2019). Adaptive control of parallel manipulator in Cartesian space. *Proceedings of the* 2019 *IEEE International Conference on Electrical, Computer and Communication Technologies* (*ICECCT*). Coimbatore, India, 1-8.

43. Al-Azzawi, R.S.; and Simaan, M.A. (2021). On the selection of leader in Stackelberg games with parameter uncertainty. *International Journal of Systems Science*, 52(1), 86-94.
44. Al-Azzawi, R.S.; and Simaan, M.A. (2019). Leader-follower controls in systems with two controllers. *Proceedings of the* 2019 *SoutheastCon*, Huntsville, USA, 1-6.
45. Humaidi, A.J.; Hameed, A.H.; and Hameed, M.R. (2018). Robust adaptive speed control for DC motor using novel weighted E-modified MRAC. *Proceedings of the* 2017 *IEEE International Conference on Power, Control, Signals and Instrumentation Engineering* (*ICPCSI*), Chennai, India, 313-319.
46. Al-Azzawi, R.S.; and Simaan, M.A. (2018). Sampled closed-loop control in multi-controller multi-objective control systems. *Proceedings of the SoutheastCon*, Petersburg, FL, USA, 1-7.
47. Marini, F.; and Walczak, B. (2015). Particle swarm optimization (PSO). A tutorial. *Chemometrics and Intelligent Laboratory Systems*, 149(Part B), 153-165.
48. Hassan, R.F.; Ajel, A.R.; Abbas, S.J.; and Humaidi, A.J. (2022). FPGA based HIL co-simulation of 2DOF-PID controller tuned by PSO optimization algorithm. *ICIC Express Letters*, 16(12), 1269-1278.
49. Humaidi, A.J.; Oglah, A.A.; Abbas, S.J.; and Ibraheem, I.K. (2019). Optimal augmented linear and nonlinear PD control design for parallel robot based on PSO tuner. *International Review on Modelling and Simulations*, 12(5)., 281-291.
50. Poli, R.; Kennedy, J.; and Blackwell, T. (2007). Particle swarm optimization: An overview. *Swarm Intelligence*, 1(1), 33-57.
51. Humaidi, A.J., Kadhim, S.K., Gataa, A.S. (2022). Optimal adaptive magnetic suspension control of rotary impeller for artificial heart pump. *Cybernetics and Systems*, 53(1), 141-167.
52. Al-Qassar, A.A.; Al-Obaidi, A.S.; Hasan, A.F.; Humaidi, A.J.; Nasser, A.R.; Alkhayyat, A.; and Ibraheem K.I. (2021). Finite-time control of wing-rock motion for delta wing aircraft based on whale-optimization algorithm. *Indonesian Journal of Science & Technology*, 6(3), 441-456.
53. Ghanim, T.; Ajel, A.R.; and Humaidi, A.J. (2020). Optimal fuzzy logic control for temperature control based on social spider optimization. *IOP Conference Series*: *Materials Science and Engineering*, 745(1), 012099.
54. Oglah, A.A.; and Msallam, M.M. (2022). Real-time implementation of Fuzzy Logic Controller based on chicken swarm optimization for the ball and plate system. *International Review of Applied Sciences and Engineering*, 13, 263-271.
55. Al-Azza, A.A.; Al-Jodah, A.A.; and Harackiewicz, F.J. (2015). Spider monkey optimization: a novel technique for antenna optimization. *IEEE Antennas and Wireless Propagation Letters*, 15, 1016-1019.
56. Al-Qassar, A.A.; Abdu-Alkareem, A.I.; Hasan, A.F.; Humaidi, A.J.; Ibraheem, K.I.; Azar, A.T.; and Hameed, A.H. (2021). Grey-wolf optimization better enhances the dynamic performance of roll motion for tail-sitter VTOL aircraft guided and controlled by STSMC. *Journal of Engineering Science and Technology* (*JESTEC*), 16(3), 1932 - 1950.
57. Abood, L.H.; Oleiwi, B.K.; Humaidi, A.J.; Al-Qassar, A.A.; Al-Obaidi, A.S.M. (2023). Design a robust controller for congestion avoidance in TCP/AQM system. *Advances in Engineering Software*, 176, 103395.

58. Abdul-Kareem, A.I.; Hasan, A.F.; Al-Qassar, A.A.; Humaidi, A.J.; Hassan R.F.; Ibraheem, I.K.; and Azar, A.T. (2022). Rejection of wing-rock motion in delta wing aircrafts based on optimal LADRC schemes with butterfly optimization algorithm. *Journal of Engineering Science and Technology* (*JESTEC*), 17(4), 2476-2495.
59. Al-Obaidi, A.S.M.; Al-Qassar, A.A.; Nasser, A.R.; Alkhayyat, A.; Humaidi, A.J.; and Ibraheem, I.K. (2021). Embedded design and implementation of mobile robot for surveillance applications. *Indonesian Journal of Science & Technology*, 6(2), 427-440.
60. Humaidi, A.J.; and Kadhim, T.M. (2018). Spiking versus traditional neural networks for character recognition on FPGA platform. *Journal of Telecommunication, Electronic and Computer Engineering*, 10(3), 109-115.
61. Suha, S.; Husain; Kadhim, M.Q.; Al-Obaidi, A.S.M.; Hasan, A.F.; Humaidi, A.J.; Al-Husaeni, D.N. (2023). Design of robust control for vehicle steer-by-wire system. *Indonesian Journal of Science & Technology*, 8(2), 197-216.
62. Hassan, R.F. (2021). Performance investigation of digital lowpass IIR filter based on different platforms. *International Journal of Electrical and Computer Engineering Systems*, 12(2), 105-111.